DC Link Control for Trains with Onboard Energy Storage using Voltage Level Signalling

Saad Ahmad
University of Oviedo, Spain
ORCID: 0009-0002-6940-4313

Mariam Saeed
University of Oviedo, Spain
ORCID: 0000-0002-0002-3072

Juan M. Guerrero
University of Oviedo, Spain
ORCID: 0000-0001-5529-9837

Iker Muniategui
Ingeteam Power Technology, Spain
iker.muniategui@ingeteam.com

Guillermo Nuñez
Ingeteam Power Technology, Spain
guillermo.nunez@ingeteam.com

David Ortega
Ingeteam Power Technology, Spain
david.ortega@ingeteam.com

Fernando Briz
University of Oviedo, Spain
ORCID: 0000-0002-6658-8746

***Abstract*—This paper addresses DC link voltage control for railway traction chains with onboard energy storage. Methods reported in the literature for DC microgrids are first studied. From this analysis, a new priority based control, which is derived from voltage level signalling method, is proposed. Simulation is used to validate the compliance of the method with all the requirements for train DC bus with onboard energy storage. Experimental results with a downscaled prototype of the system are provided to validate the method.**

***Index Terms*—DC link control, On board energy storage, Regenerative braking energy**

I. Introduction

Electric trains are a major means of transportation nowadays. Recently trains with onboard energy storage are getting importance due to their advantages like peak shaving, stabilization of catenary voltage, last mile functionalities and catenary free operation for sometime. In addition, regenerative braking energy can be stored and reused later[1][2].

DC link control is an important part for stability and power flow controllablity of such systems[3]. Traction chain with onboard energy storage can be considered a special micro grid with some different features. The requirements for the traction chain can change from case to case; for the system discussed in this paper, these requirements are:

- It should be able to share power between different energy sources for optimized operation.
- System should be able to prioritize different energy sources.
- Large variations in DC bus voltage are not allowed.
- It is desirable that the control structure remains the same independent of the mode of operation (i.e. of the power sources available and of the loads at any time).

Literature on DC link control is widely available for DC and AC micro grids. Droop control based methods are widely used for bus voltage control with distributed energy resources [4–6]. Most of them have been proven to be very effective thanks to their power sharing capabilities, and are able to guarantee controlability of bus voltage in micro grids. But they lack ability to prioritize the energy sources properly or need major modifications for doing so. Therefore they are not especially well suited for their use in on-board DC microgrids.

DC bus signalling based methods have also been proposed in literature for controlling DC bus voltage [7–9]. They have the advantage over droop control of easiness for setting priorities for sources; however, this can be at the cost of relatively large variations in the DC bus voltage, as every energy source will *block* a certain voltage range for its operation. Further, these methods also lack the capability of power sharing.

A third group of methods studied in literature combine advantages of droop based and DC bus signalling based methods. However, they require changes in the control structure depending on the mode of operation [10–12]. As explained before, this feature is not desirable.

To summarize, the above discussed methods have one or more of the following limitations:

- Only applicable for operation where large variations in DC bus voltage are allowed.
- Assigning priorities to power sources is not possible.
- Change in control structure for different operation modes is required.

This paper proposes a novel control strategy which can prioritize energy sources along with the capability of maintaining constant DC bus voltage in steady state for train with onboard energy storage. The proposed control method avoids change in control structure during mode transition for smooth operation. It will be shown that the proposed method meets system's requirements in all modes of operation. The paper is organized as follows:

Section II explains structure of the system under study, its various parts and different modes of operation. Section III and IV explains the working of the proposed control and its

This work was supported in part by the European Commission HORIZON and KDTJU under project POWERIZED GA No 101096387 and in part by the Spanish Ministry of Science and Innovation under grant MCINN-23-PCI2022-135021-2.

validation in simulation respectively. Experimental results and conclusions are discussed in section V and VI respectively.

II. System's Description

The general block diagram of an electric train with onboard energy storage is shown in Fig. 1. Main parts of the traction chain are described as following.

A. Energy sources and loads

Main sources and loads in train with onboard energy storage are catenary, energy storage, traction motor and auxiliary loads. They are briefly discussed below.

- Catenary: It is an overhead line along the track to supply electrical energy to the train. It can be DC or AC. Usually a DC catenary is directly connected to the DC link via an LC filter. For AC catenary an isolation transformer is connected which collects power from the catenary, steps down the voltage level and supply it to the DC link via active front end (AFE) converter. In this paper it is modelled as a DC source as shown in Fig. 1.
- Energy storage device: It can be of different types like battery storage, fuel cell etc. It can supply power for traction at peak loads or when there is no catenary available. It is also used to store braking energy for later reuse. As the power flow is bidirectional, it can be considered both source and load depending on the direction of power flow.
- Traction drive provides the required traction force to the train. Most of the time it works as a motor, and therefore consumes energy form the DC link. However, it can also work as a source at times of braking and can provide power to be used for other loads. In this paper 3-phase induction motor is considered and will be used for simulations.
- Auxiliary loads like lighting, air conditioning, as well as pumps, fans, etc. also consume considerable part of the energy. In this paper it is considered as a resistor connected across DC bus for simplicity.

B. Power converters

Power converters normally used in trains are AFEs, traction inverters and auxiliary converters. For the case of trains with onboard energy storage, a DC/DC converter is normally used to interface the energy storage elements with the DC link [13]. A brief description of the power converters is given following:

- AFE : It is a bidirectional AC-DC converter which collects power from the catenary and feeds it to the DC bus. In this paper a DC-DC converter is considered for simplicity of Simulink model but the concept proposed in this paper will work the same for a system with AC catenary and AFE. Generally cascaded voltage and current control is used for such converters. Current control used in this paper is shown in Fig. 2a.
- Energy storage converter: It is a DC-DC converter which controls the power flow between energy storage and DC bus. General typologies used for this purpose are buck/boost converters. In this paper 3 level converter is used for system simulations. Generally cascaded voltage and current control is used for such converters. Fig. 2b shows the current control loop used in this paper.
- Traction inverter: It is a 3 phase inverter connected to the DC bus. It supplies power to the traction motor. Generally scalar or vector controls are used for such type of inverters. In this paper field oriented control is used for simulation which is shown in the Fig. 2c.
- Auxiliary converter: Depending on the types of loads, it can be one or more single-phase or/and 3-phase inverters.

C. Modes of operation

Depending on availability of energy sources, the system considered in this paper have three modes of operation: mixed, catenary only and energy storage only. They are shown in Fig. 3.

- Mixed mode: This is the most general operating mode. Both catenary and energy storage are available. Catenary is used as the first priority source for power consumption. For the case discussed here, the line converter is not rated to supply the peak load, therefore onboard energy storage system must contribute to the extra power when required. Other possible reason for the combined use of catenary and energy storage systems is in the event of a weak catenary (it is noted that railway standards allow a decrease of the catenary voltage to 66% of its nominal value). During braking, the regenerative energy produced is used for auxiliary loads, battery charging and feeding back to the catenary as a first, second and last priorities.
- Catenary only mode: In this mode only catenary is available. This can happen due to fully discharged energy storage or unavailability of energy storage. In this mode, catenary is the main source to provide power to the auxiliary loads and also for traction. During braking, the regenerative energy produced is used for auxiliary loads as a first priority. If it is more than auxiliary loads, the rest is fed back to the catenary.
- Energy storage only mode: In this mode only energy storage is available. This can happen due to fault in catenary or when the train is passing through a zone where catenary is not feasible. Energy storage is responsible for supplying power to auxiliary loads as well as traction. During braking, the regenerative energy can be used for auxiliary loads. If it is more than auxiliary loads, the rest is used for energy storage charging.

III. Proposed DC link control using voltage level signalling

The use of DC bus voltage signalling for DC link control of the train is proposed in this section. The method is an adapted version of DC bus signalling method which is already used in micro grids [14]. Therefore it is briefly explained here.

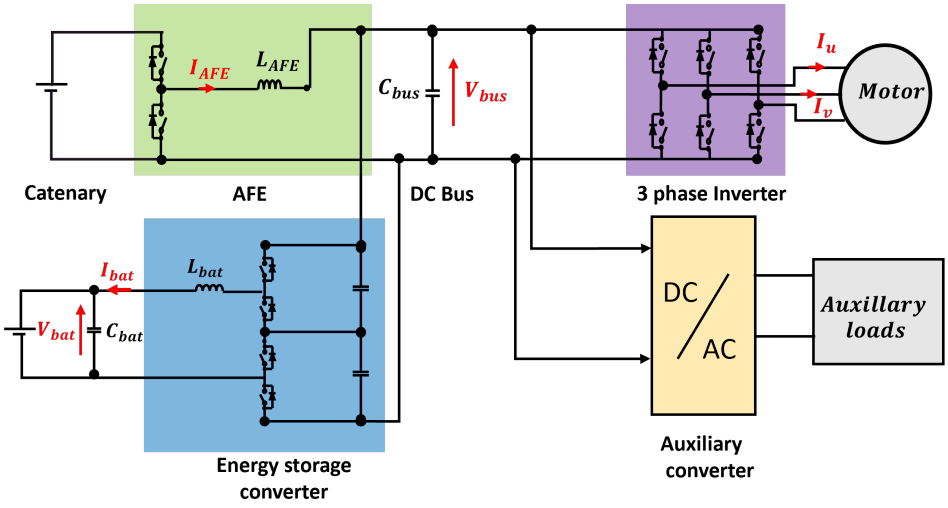

Fig. 1: Traction chain and loads of an electric train with OESS

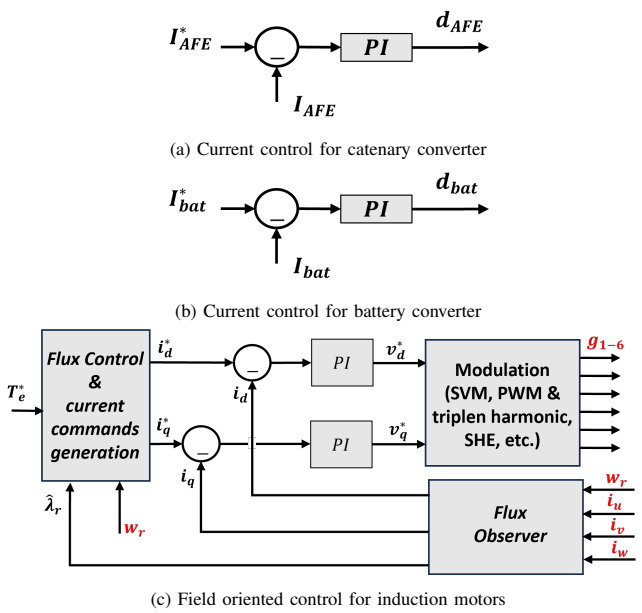

(a) Current control for catenary converter

(b) Current control for battery converter

(c) Field oriented control for induction motors

Fig. 2: Control structures for different power converters

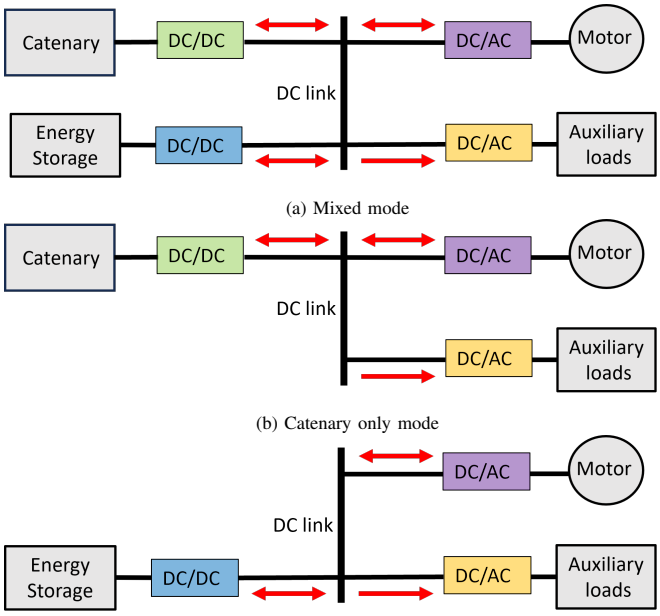

(a) Mixed mode

(b) Catenary only mode

(c) Energy storage only mode

Fig. 3: Different modes of operation. Red arrows show the possible directions of power in each mode.

A. DC bus voltage level signalling method

A distinguishing feature of this method is that it naturally utilizes the saturation limits of inner current control loops to set priorities of the sources. It is specially suited for applications where relatively large variations in DC bus are allowed. With increase in load current controller naturally saturates and the DC bus voltage drops down activating the next current controller. With increasing load, current controllers saturates one after another and next controller activates to regulate the DC bus voltage. Fig. 4 shows the behaviour of DC bus voltage and powers of different energy sources with increasing load.

B. Proposed priority based DC link control

Block diagram of the proposed DC link control is shown in Fig. 5. Its most distinguishing features are as follows.

Large variations in DC bus voltage are not allowed. However, voltage variations are an intrinsic requirement of bus signalling based methods. To solve this conflict, a secondary voltage regulation loop was added to guarantee that the DC bus voltage remains constant.

Reference command I^{**}_{bat} should be followed when enough power is available from catenary, what in first instance is in conflict with the catenary having priority over power sources. To harmonize both requirements, a summer block is added to

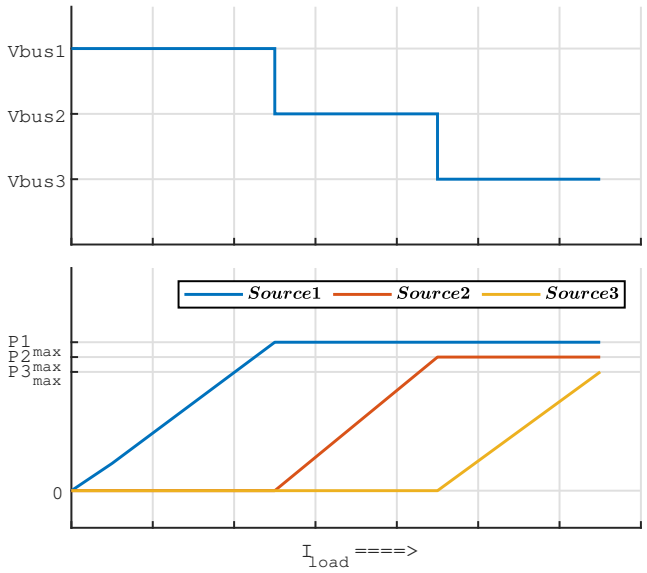

Fig. 4: DC bus voltage level signalling method

output of the PI_{Bat}. It guarantees that reference command I_{bat}^{**} is followed when PI_{Bat} is saturated at 0.

Reference torque command T_e^{**} should be followed when there is enough power available from catenary and battery. A summer block is added to output of the PI_{IM}. It makes sure reference command T_e^{**} is followed when PI_{IM} is saturated at 0.

At a time one voltage PI controller is activated and regulates the DC link voltage. Other two PI controllers are saturated at their maximum or minimum values. When PI_{AFE} saturates, it clamps its power to the maximum. DC bus voltage drops down and crosses the next voltage level. Second priority power source starts regulating the DC bus voltage. Secondary voltage PI controller PI_V starts to adjust the reference by adding ΔV_{bus}^* to maintain the DC bus voltage. Similarly when the load is increased, PI_{Bat} also saturates at maximum power. DC bus drops down and the error signal to PI_{IM} becomes positive and it starts regulating the voltage by adjusting the torque command.

Saturation limits of all the converters can be changed when needed. It could happen due to strong or weak catenaries, low or high state of charge of energy storage and optimized operation. Priorities are set by setting reference bus voltage levels V_{bus}^*1 , V_{bus}^*2, V_{bus}^*3. The higher the reference bus voltage level the higher is the priority of the source. For this application catenary is the first priority source, then battery and then the kinetic energy of train during power consumption. There are three scenarios that can happen depending on the available and required power from different energy sources and loads.

1) AFE regulates the DC bus voltage. Power inequality (1) holds in this case.

$$P_{cat} > P_{aux} + P_{motor} + P_{bat} \tag{1}$$

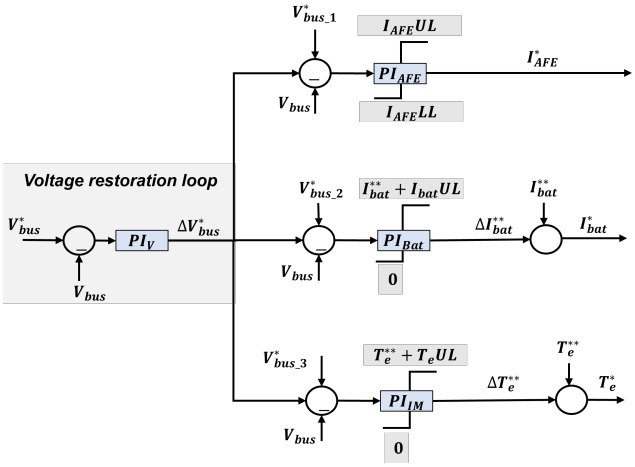

Fig. 5: Proposed priority based control

PI_{Bat} and PI_{IM} saturate to 0. I_{bat}^{**} and T_e^{**} commands are followed.

2) Battery converter regulates the DC bus voltage. Power inequality (2) holds in this case.

$$P_{cat} + P_{bat} > P_{aux} + P_{motor} \tag{2}$$

PI_{AFE} and PI_{IM} saturates at maximum and 0 respectively. Torque command T_e^{**} command is followed.

3) PI_{IM} regulates the DC bus voltage. Power inequality (3) holds in this case.

$$P_{cat} + P_{motor} + P_{bat} > P_{aux} \tag{3}$$

PI_{AFE} and PI_{Bat} saturate at their maximum.

IV. Simulation Results

To validate the method, two different Simulink models of all converters shown in Fig. 1, including loads and controls, are developed. These models, namely the switching model and averaged mode, are described following.

A. Switching simulation model

Its objective is to model the system behavior at the switching-time scale, to be able reproduce with a reasonable accuracy switching events and their interactions with the controls, as well as possible high frequency events when the control changes the mode of operation.

Different scenarios are created to validate the control method. Results are shown in Fig. 6. The modes of operation shown in this figure are:

1) $t = 0-2$ secs $\Rightarrow$ Peak load. Power inequality (4) applies.

$$P_{cat} + P_{bat} > P_{aux} + P_{motor} \tag{4}$$

PI_{AFE} is saturated. Catenary is operating at its maximum limit. Battery provides the rest of the power to regulate the DC bus voltage.

2) $t = 2-5$ secs $\Rightarrow$ Battery disconnected or fully discharged. Power inequality (5) applies.

TABLE I: Simulation parameters

	Parameter	Symbol	Value
DC Supply	Supply voltage	V_{supply}	5000 V
2 level DC-DC converter	Filter inductance	L_{2L}	$360uH$
Battery	Voltage	V_{bat}	1800V
3 level DC-DC converter	Filter inductance	L_{3L}	$32.6uH$
Induction motor	Rated Power	–	8500 kW
	RPM	–	1670 rpm
Locomotive	mass	m	400 ton
	Wheel's radius	r_w	0.55 m
Auxiliary load	Auxiliary power	P_{aux}	360 kW
Voltage references	AFE	$V^*_{bus_1}$	3600 V
	Battery	$V^*_{bus_2}$	3550 V
	Traction inverter	$V^*_{bus_3}$	3500 V

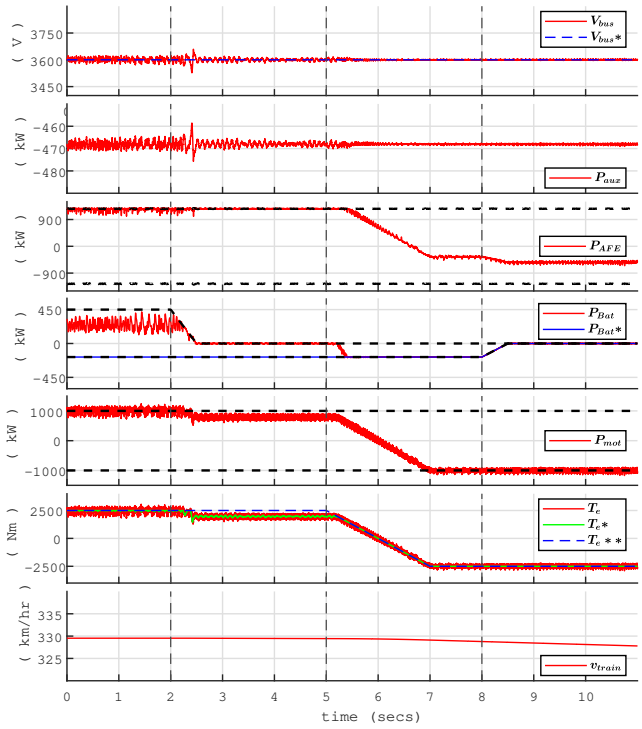

Fig. 6: Simulation results with switching model. Dashed lines show power limits of each converter

$$P_{cat} + P_{bat} + P_{motor} > P_{aux} \tag{5}$$

Battery power limit is decreased to 0. It results in saturation of PI_{Bat} and PI_{IM} is activated. PI_{IM} regulates the DC bus by adjusting the traction effort which results in decrease in speed. As the time scale is in seconds, therefore due to high inertia of train decrease in speed is negligible.

3) $t = 5 - 8$ secs $\Rightarrow$ Braking. Power inequality (6) applies.

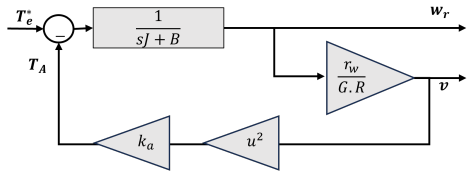

(a) Simplified train dynamic model

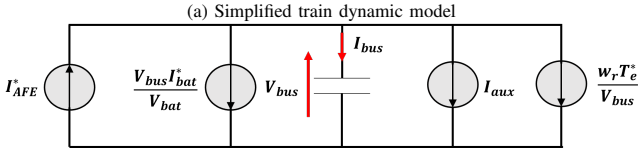

(b) Simplified DC bus average model

Fig. 7: Average model of the system

$$P_{cat} > P_{bat} + P_{motor} + P_{aux} \tag{6}$$

Train brakes which could be the case when train is about to reach its destination. The regenerative braking energy is fed back into the DC link. DC bus voltage goes high and pass $V^*_{bus}1$ which activates PI_{AFE}. PI_{AFE} starts regulating the DC bus voltage. Battery has also started charging due to excess of power.

4) $t = 8{-}11$ secs $\Rightarrow$ Battery fully charged. Power inequality (4) applies.

$$P_{cat} > P_{aux} + P_{motor} + P_{bat} \tag{7}$$

Battery charging command is set to zero which could be the case when battery is fully charged. Braking energy is more than the auxiliary load so catenary starts absorbing the extra energy and regulates the DC bus voltage.

B. Average simulation model

The effect of some modes of operation of the proposed DC link voltage control will affect to speed of the train. Due to high inertia of train, changes in train speed can only be seen in long simulations. Use of switching model would be prohibitive in this case due to both time and computational requirements. An average of the system was developed to see the long-term response. Parameters used for simulation are similar to those of a real train, they are given in Table. I.

Average model for the system is shown in Fig. 7. The mechanical model (Fig. 7a) corresponds to a first order inertia-friction system, with aerodynamic friction. The average model of the DC link is shown in Fig. 7b. It is assumed that the inner control loops are faster and follow the commands instantaneously. Power converters are replaced by current sources under this assumption.

Different scenarios are created to validate the control strategy and results are shown in Fig. 8.

1) $t = 0 - 10$ mins $\Rightarrow$ Strong catenary. Power inequality (12) applies.

$$P_{cat} > P_{aux} + P_{motor} + P_{bat} \tag{8}$$

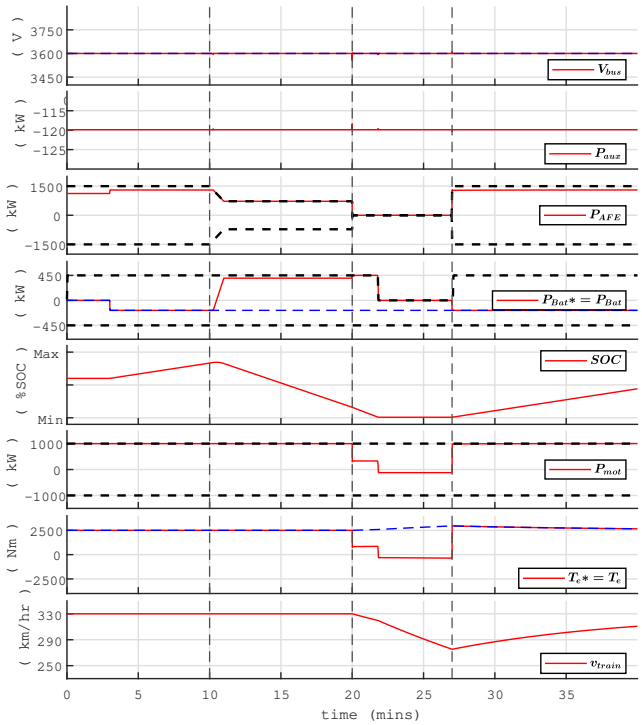

Fig. 8: Simulation results for different scenarios using average model.

$\Rightarrow$ Catenary is providing power to auxiliary load and motor. Train is moving at a constant speed of 330 km/hr. Battery started charging at $t = 3$ mins, which results in SOC increase. Catenary can still manage to provide power to all the loads and is regulating DC bus voltage.

2) $t = 10 - 20$ mins $\Rightarrow$ Weak catenary. Power inequality (13) applies.

$$P_{cat} + P_{bat} > P_{aux} + P_{motor} \tag{9}$$

Catenary max power limit is decreased which could be the case if catenary is weak. PI_{AFE} has saturated and catenary power clamps at the maximum limit. Battery starts to provide the rest of the power to regulate the DC bus voltage, which results in decrease in SOC.

3) $t = 20 - 27$ mins $\Rightarrow$ Catenary disconnected. Power inequality (14) applies.

$$P_{cat} + P_{bat} + P_{motor} > P_{aux} \tag{10}$$

Catenary max power limit is set to 0 which could be the case when catenary is disconnected. PI_{Bat} saturates and battery power clamps at the maximum limit. Train decreases its traction effort to regulate the DC bus voltage which results in decrease in speed. At $t = 22$ mins, battery is fully discharged and no more available to feed the power. Motor starts feeding the power back to regulate the DC bus voltage. As kinetic energy of train is used in doing so, speed starts to decrease at a more faster rate.

4) $t = 27 - 40$ mins $\Rightarrow$ Catenary re-connection. Power inequality (15) applies.

TABLE II: Test bench parameters

		Parameter	Symbol	Value
DC catenary	DC supply	Supply voltage	V_{supply}	350 V
	2L dc-dc converter	Filter inductance	L_{AFE}	3.96 mH
		Series resistance	R_{AFE}	0.6 Ω
Energy storage system	Battery	Voltage	V_{bat}	200 V
	3L dc-dc converter	Filter inductance	L_{AFE}	1.11 mH
		Series resistance	R_{bat}	0.2 Ω
		Output capacitor	$C_{out_{bat}}$	550 µF
Traction drive system	Induction motor	Rated Power	–	1.32 kW
		RPM	–	1670 r/min
DC bus		Capacitance	C_{bus}	550 µF
Auxiliary load		Resistor	R_{aux}	100 Ω

$$P_{cat} > P_{aux} + P_{motor} + P_{bat} \tag{11}$$

Catenary is connected again and is regulating the DC bus voltage by supplying power to all the loads. Battery starts to charge again, its SOC going up. Speed of the train starts to increase again. I_{bat}^{**} and T_e^{**} command is followed.

The simulation results do not include the response of control for change in reference bus voltage as this is not required in practice. In case of DC catenary connected directly to the DC link, the bus voltage will change with the catenary voltage. It is noted that all the control concepts discussed in this paper remain valid in this case too.

V. Experimental Validation

A down scaled prototype of a traction chain with onboard energy storage shown in fig. 1 was built to validate the proposed method. Parameters of the testbench are given in Table. II. Fig 9 shows the experimental results, the modes of operation of the control being explained as under.

1) $t = 0 - 5$ seconds $\Rightarrow$ Strong catenary. Power inequality (12) applies.

$$P_{cat} > P_{aux} + P_{motor} + P_{bat} \tag{12}$$

Catenary is providing power to auxiliary load and motor. Motor is running at targeted speed (314 rad/s). Battery is charging at 1.5 amperes. Catenary is regulating DC bus voltage.

2) $t = 5 - 10$ seconds $\Rightarrow$ Weak catenary. Power inequality (13) applies.

$$P_{cat} + P_{bat} > P_{aux} + P_{motor} \tag{13}$$

Catenary max current limit is decreased due to the weak catenary. PI_{AFE} clamps catenary at its power limit. Battery starts to provide the needed power to regulate the DC bus voltage.

3) $t = 10 - 13$ seconds $\Rightarrow$ Battery discharged. Power inequality (14) applies.

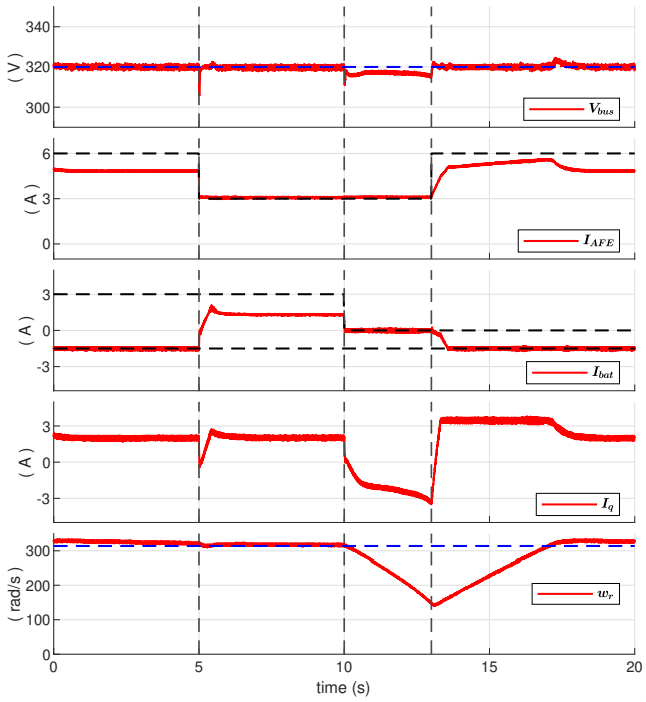

Fig. 9: Experimental results for different scenarios. Black and blue dashed lines show current limits and reference commands respectively of each converter.

$$P_{cat} + P_{bat} + P_{motor} > P_{aux} \tag{14}$$

Battery discharge current limit is decreased to zero to emulate a fully discharged battery. Hence it is not available anymore to feed the power. Motor starts braking, feeding the power back to regulate the DC bus voltage. Consequently train speed decreases.

4) $t = 13-20$ seconds $\Rightarrow$ Strong catenary recovered. Power inequality (15) applies.

$$P_{cat} > P_{aux} + P_{motor} + P_{bat} \tag{15}$$

Catenary current limit is increased again which results in its ability to supply power to all the loads and is regulating the DC bus voltage. Train speed recovers and battery resumes charging.

VI. Conclusions

This paper address the DC link voltage control of trains including onboard energy storage systems. Though the use of methods developed for DC microgrids is possible, its application to the train case is not straightforward due the peculiarities of the system.

A new DC link control method using bus signalling has been proposed in this paper. The proposed method allows priority assignments to the available power sources, while avoiding permanent deviations of the DC link control with respect to its nominal value. Further, the proposed method avoids change in control structure due to changes in the operation mode. The proposed control is validated in Simulink/Matlab, complying with the requirements in all modes of operation.

Finally, experimental results using a down scaled model of the system have been provided, confirming the viability of the proposed control strategy.

References

[1] X. Liu and K. Li. "Energy storage devices in electrified railway systems: A review". In: *Transportation Safety and Environment* 2.3 (July 2020), pp. 183–201. ISSN: 2631-4428. DOI: 10.1093/tse/tdaa016. eprint: https://academic.oup.com/tse/article-pdf/2/3/183/34057407/tdaa016.pdf. URL: https://doi.org/10.1093/tse/tdaa016.

[2] Z. Liu, M. Berg, and A. Ekmark. "Conceptual exploration of power peak shaving by smart train operation in rail freight transport". In: *Proceedings of the Institution of Mechanical Engineers, Part F: Journal of Rail and Rapid Transit* 236.7 (2022), pp. 838–849. DOI: 10.1177/09544097211045544.

[3] W. Chen, X. Ruan, H. Yan, and C. K. Tse. "DC/DC Conversion Systems Consisting of Multiple Converter Modules: Stability, Control, and Experimental Verifications". In: *IEEE Transactions on Power Electronics* 24.6 (2009), pp. 1463–1474. DOI: 10.1109/TPEL.2009.2012406.

[4] J. M. Guerrero, J. C. Vasquez, J. Matas, L. G. de Vicuna, and M. Castilla. "Hierarchical Control of Droop-Controlled AC and DC Microgrids—A General Approach Toward Standardization". In: *IEEE Transactions on Industrial Electronics* 58.1 (2011), pp. 158–172. DOI: 10.1109/TIE.2010.2066534.

[5] M. Shahbazi, B. Kazemtabrizi, and C. Dent. "Coordinated control of DC voltage magnitudes and state of charges in a cluster of DC microgrids". In: *2016 IEEE PES Innovative Smart Grid Technologies Conference Europe (ISGT-Europe)*. 2016, pp. 1–5. DOI: 10.1109/ISGTEurope.2016.7856272.

[6] X. Yang, H. Hu, Y. Ge, S. Aatif, Z. He, and S. Gao. "An Improved Droop Control Strategy for VSC-Based MVDC Traction Power Supply System". In: *IEEE Transactions on Industry Applications* 54.5 (2018), pp. 5173–5186. DOI: 10.1109/TIA.2018.2821105.

[7] F. Li, Z. Lin, H. Xu, and R. Wang. "A Review of DC Bus Signalling Control Methods in DC Microgrids". In: *2022 IEEE International Power Electronics and Application Conference and Exposition (PEAC)*. 2022, pp. 1286–1291. DOI: 10.1109/PEAC56338.2022.9959577.

[8] J. Bryan, R. Duke, and S. Round. "Decentralized generator scheduling in a nanogrid using DC bus signaling". In: *IEEE Power Engineering Society General Meeting, 2004.* 2004, 977–982 Vol.1. DOI: 10.1109/PES.2004.1372983.

[9] K. Sun, L. Zhang, Y. Xing, and J. M. Guerrero. "A Distributed Control Strategy Based on DC Bus Signaling for Modular Photovoltaic Generation Systems With Battery Energy Storage". In: *IEEE Transactions on Power Electronics* 26.10 (2011), pp. 3032–3045. DOI: 10.1109/TPEL.2011.2127488.

[10] C. Jin, P. Wang, J. Xiao, Y. Tang, and F. H. Choo. "Implementation of Hierarchical Control in DC Microgrids". In: *IEEE Transactions on Industrial Electronics* 61.8 (2014), pp. 4032–4042. DOI: 10.1109/TIE.2013.2286563.

[11] D. Wu, F. Tang, T. Dragicevic, J. M. Guerrero, and J. C. Vasquez. "Coordinated Control Based on Bus-Signaling and Virtual Inertia for Islanded DC Microgrids". In: *IEEE Transactions on Smart Grid* 6.6 (2015), pp. 2627–2638. DOI: 10.1109/TSG.2014.2387357.

[12] L. Wu, J. Zeng, H. Cheng, and Q. Ren. "A DC Bus Signaling Based Autonomous Power Management Strategy for a Grid-connected PV-Battery System". In: *2019 IEEE 10th International Symposium on Power Electronics for Distributed Generation Systems (PEDG)*. 2019, pp. 628–633. DOI: 10.1109/PEDG.2019.8807712.

[13] M. Saeed, F. Briz, J. M. Guerrero, I. Larrazabal, D. Ortega, V. Lopez, and J. J. Valera. "Onboard Energy Storage Systems for Railway: Present and Trends". In: *IEEE Open Journal of Industry Applications* 4 (2023), pp. 238–259. DOI: 10.1109/OJIA.2023.3293059.

[14] J. Bryan, R. Duke, and S. Round. "Decentralized control of a nanogrid". In: *Int. Power Eng. Conf.* 14 (Jan. 2005), pp. 39–44.